

Journal of Materials Chemistry B

Accepted Manuscript



This is an *Accepted Manuscript*, which has been through the Royal Society of Chemistry peer review process and has been accepted for publication.

Accepted Manuscripts are published online shortly after acceptance, before technical editing, formatting and proof reading. Using this free service, authors can make their results available to the community, in citable form, before we publish the edited article. We will replace this *Accepted Manuscript* with the edited and formatted *Advance Article* as soon as it is available.

You can find more information about *Accepted Manuscripts* in the [Information for Authors](#).

Please note that technical editing may introduce minor changes to the text and/or graphics, which may alter content. The journal's standard [Terms & Conditions](#) and the [Ethical guidelines](#) still apply. In no event shall the Royal Society of Chemistry be held responsible for any errors or omissions in this *Accepted Manuscript* or any consequences arising from the use of any information it contains.

Thromboresistant and rapid-endothelialization effects of dopamine and staphylococcal protein A mediated anti-CD34 coating on a 316L

Stainless Steel for cardiovascular devices

Jialong Chen ^{a,b*}, Quanli Li ^a, Jianguang Xu ^a, Le Zhang ^a, Manfred F. Maitz ^c, Jun Li ^{b*}

^a *Stomatologic Hospital & College; Anhui Medical University, Key Lab. of Oral Diseases Research of Anhui Province, Hefei 230032, China*

^b *College of pharmacy; Anhui Medical University, Hefei 230032, China*

^c *Leibniz Institute of Polymer Research Dresden, Max Bergmann Center of Biomaterials Dresden, Dresden 01069, Germany*

* Corresponding author.

Jialong Chen

Tel/Fax: +86-551-65161183

E-mail address: jialong_dt@126.com

Jun Li

Tel/Fax: +86-551-65161183

E-mail address: lijun@ahmu.edu.cn

Abstract:

There is convincing evidence in vivo that the vascular homing of endothelial progenitor cells (EPCs) contributes to a rapid endothelial regeneration, which could prevent thrombosis and restenosis of cardiovascular devices. To enhance the EPC homing on cardiovascular devices, immobilization of an EPC capture agent (e.g. an anti-CD34 antibody) on the surface of cardiovascular devices is critical. We describe a way of immobilizing anti-CD34 Ab onto 316L Stainless Steel (316L SS). For this, surface modification of 316L SS was developed via self-polymerization of dopamine (DA) and covalent grafting of staphylococcal protein A (SPA). On this coating the anti-CD34 Ab were oriented immobilized through their Fc constant region with SPA. In this process, the results of quartz crystal microbalance, X-ray photoelectron spectroscopy and water contact angle indicate that DA, SPA and anti-CD34 Ab were successfully immobilized onto the surface step by step. In vitro blood-compatibility tests confirmed that the modified surface induced less pro-coagulant fibrinogen denaturation, less platelet adhesion and lower activation of the adherent platelets. The affinity of EPC to the modified surface has been demonstrated under flow condition. This study provides potential application for cardiovascular implant materials.

Key word: Endothelial progenitor cells; Dopamine; Staphylococcal protein A; Anti-CD34 antibody; Rapid-endothelialization

Introduction

Many cardiovascular and other blood contacting biomedical devices have been widely applied, such as vascular stents, vascular grafts, artificial heart valves, or blood pumps¹, and contribute significantly to the quality and effectiveness of the health care system. However, in the environment of blood, complications such as blood clotting and thrombus formation or, in the case of vascular stents, proliferation of smooth muscle cells and restenosis frequently lead to the failure of the device. Surface engineering is required to provide improved passive or active hemocompatible properties².

Permanent medical devices in the blood stream are prone to thrombus formation on their surface, which hinders rapid and complete coverage of the device by endothelial cells (EC). EC, physiologically the inner lining of blood vessels, are desired to colonize a biomedical device, because they exhibit anticoagulant and anti-adhesive properties for blood platelets and

leukocytes³.

Restenosis is a direct consequence of vessel injury during stent implantation, fibrin deposition, infiltration with inflammatory cells with subsequent neointima formation and remodeling resulting in occlusion of the lumen³. These developments result from a persistent disturbance and delayed recovery of the endothelial cells⁴. The establishment of a functional endothelial layer soon after device implantation has been shown to be among the main factors in the prevention of restenosis and stent thrombosis⁵.

The discovery of circulating endothelial progenitor cells (EPCs)⁶ opened up revolutionary new perspectives for in vivo/in situ endothelialization of implanted blood contacting biomedical devices by capturing endogenous circulating EPCs directly from the blood. Due to the promising benefits of EPCs in regenerative medicine, several molecules, such as anti-CD34 antibodies(anti-CD34 Ab), have been immobilized on the surface of devices via electrostatic interaction⁷ or by covalent immobilization⁸⁻¹⁰ to attract EPCs directly from the bloodstream. These methods, however, require chemical modification of the surface, and it is not possible to control the molecular orientation of the immobilized proteins. When antibodies are immobilized on a material surface, their binding activity usually decreases. This reduced binding activity is ascribed to the random orientation and steric hindrance of the antibody molecules on the material surface¹¹. Therefore, a method for the oriented immobilization of functional antibodies is needed¹². Oriented immobilization of anti-CD34 Ab on materials through avidin-biotinylated protein A was described extensively by our group in a previous report and this coating could increase EPC attachment and capture, and induce rapid complete endothelialization of the luminal surface of the implant in vivo¹³. But the stability of coating wasn't very well because of electrostatic interaction between the coating and material. So it is very important that anti-CD34 Ab can be tightly oriented immobilized on the material surface.

Staphylococcal protein A(SPA) is a cell wall component of the bacterium *Staphylococcus aureus* that binds specifically to many mammalian immunoglobulins, most notably immunoglobulin G (IgG), via the Fc region¹⁴. The antigen-binding capacity of antibody linking with SPA does not interfere because the antigen-binding sites of antibody are located on the distal ends of the Fab variable regions¹⁵. Thus, SPA has been used for oriented immobilization of

antibody to retain its antigen-binding capacity in biosensor¹¹.

Dopamine is a small-molecule mimic of the adhesive proteins of mussels and contains unusually high concentrations of catechol and amine functional groups, which are capable of mediating protein immobilization to most organic and inorganic surfaces¹⁶⁻¹⁹.

Inspired by this discovery as well as several successful examples of using DA and SPA in molecular immobilization, we have developed a facile approach to immobilize SPA based on surface coating of 316L SS with a thin layer of DA polymerized in the presence of SPA solution, then the SPA modified surface provided an anchor for oriented immobilization of the anti-CD34 Ab (Figure 1).

The aim of the present study was to prepare the tight functional surface with dopamine, Staphylococcal protein A and anti-CD34 Ab and evaluate such surface for the capacity to capture EPCs, to resist SMCs attachment and to improve blood-compatibility.

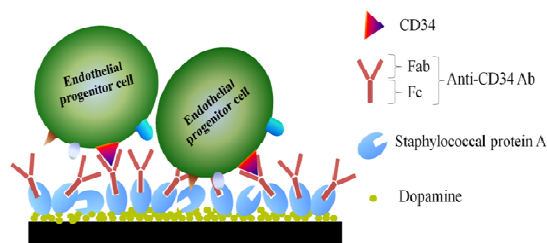


Figure 1. Ideal reaction scheme for oriented immobilization of anti-CD34 antibodies on 316L SS through dopamine and Staphylococcal protein A

2. Materials and methods

2.1 Materials

Dopamine hydrochloride, Staphylococcal Protein A (SPA), TRIS-HCl buffer base and rabbit anti-Goat IgG F(ab')₂-Peroxidase antibody were obtained from Sigma-Aldrich. Polyclonal goat anti-human-CD34 IgG and monoclonal mouse anti-human fibrinogen γ -chain were purchased from Santa cruz biotechnology Inc and Accurate chemical & Scientific Corp, respectively. Polyclonal rabbit anti-mouse antibody against actin was purchased from Beijing Zhong Shan Golden Bridge Biological Technology CO., LTD. Goat anti-human Fibrinogen IgG HRP-conjugated antibody was purchased from Beijing Biosynthesis Biotechnology Co., LTD. Monoclonal sheep anti-mouse IgG HRP-conjugated antibody, monoclonal mouse anti-human P-selectin antibody and monoclonal sheep anti-mouse IgG Cy3-conjugated antibody were

purchased from BD Biosciences, San Jose, CA. All the other reagents used in the experiments were of the highest analytical purity (>99.9%).

2.2 Method

2.2.1 Preparation and characterization of the modified surface

316L SS disks were polished to a reflective mirror-like finish. The samples were ultrasonically cleaned subsequently in a detergent solution, acetone, ethanol, and finally in ultrapurified (up) water. After cleaning, the samples were immersed in a 2 mg/mL solution of dopamine (10 mM Tris buffer, pH 8.5) for about 24 h at room temperature in the dark. Then, the samples were sonicated for 10 min in up water (three times) to remove the nonattached dopamine; the samples are denoted as SS-DA. The dopamine-modified samples were then placed in a 24 well plate and incubated with a 300 μ l aqueous solution of SPA (5 μ g/mL) at 37 °C overnight, rinsing with up water; the samples are denoted as SS-DA-SPA. The above samples were then placed in a 24 well plate and incubated with a 300 μ l aqueous solution of polyclonal goat anti-human CD34 IgG (0.1 μ g/mL) at 37 °C overnight, rinsing with up water, the samples are denoted as SS-DA-SPA-CD34.

The immobilized quantity of each component was determined by the Q-Sense E4 system (Q-Sense AB, Sweden) with a fundamental frequency of 5.0 MHz. The quartz crystal microbalance (QCM) is widely used to measure the change in mass (Δm) of molecules adsorbed on the surface of the quartz crystal via changes in the resonance frequency (Δf). The surface of gold (Au)-coated quartz crystal (diameter, 10mm) was initially treated with UV irradiation for 30 min for surface cleaning and sterilizing, then settled in the measurement chamber and 10 mM Tris buffer (pH 8.5) was injected as a buffer for equilibrium. A 2 mg/mL solution of dopamine (10 mM Tris buffer, pH 8.5) was injected at 10 μ l/min, then rinsed with up water at 100 μ l/min. Subsequently, aqueous solution of SPA (5 μ g/mL) was injected at 10 μ l/min until no variation appeared in the adsorption curves, then rinsed with up water at 100 μ l/min. Aqueous solution of polyclonal goat anti-human-CD34 IgG (0.1 μ g/mL) was injected at 10 μ l/min for building up the coating on the quartz crystal surface until no variation appeared in the adsorption curves, then rinsed with up water at 100 μ l/min for 20min. For evaluating the stability, the coating was rinsed with up water at 500 μ l/min for 24hour. Measurements were all conducted at a temperature of 37°C. Q-Tools software (Q-Sense AB, Gothenburg, Sweden) was used to analyze the QCM data

and to extract quantitative parameters of the adsorption of each component on the surface of the quartz crystal at 5th overtone of the fundamental resonant frequency.

The surface composition of the samples was analyzed by X-ray photoelectron spectroscopy (XPS, Perkin Elmer 16PC) with an Al Ka X-ray source (1486.6 eV photons). A wide-scan survey spectrum over a binding energy (BE) range of 0–1400 eV was recorded at pass energy of 80 eV for estimation of the chemical elemental composition and 10 eV for high-resolution detailed scans. The system was calibrated using the C1s peak at 284.8 eV. All spectra were recorded at a take-off angle of 15 degree. The maximum information depth of the XPS method is not more than 10 nm. In order to determine the quantitative surface composition from XPS data, spectrum background was subtracted according to the Shirley method. The parameters of the component peak fitting were their binding energy, height, full width at half maximum, and the Gaussian–Lorentzian ratio.

Water contact angle analysis was performed with DSA100 drop shape analysis system (DSA100, Krüss, Germany) using up water at room temperature. Five samples were measured of each group, and two separate measurements were made on each sample.

The amount of F(ab') fragments exposure of anti-CD34 Ab on the surface was determined by enzyme-linked immunosorbent assay (ELISA) as follows: (i) Samples were immersed in 1% sheep serum for 60 min to block non-specific adsorption, then the solution was decanted; (ii) 20 μ m of rabbit anti-Goat IgG F(ab')₂-Peroxidase antibody(1:100) were added to the surface of the samples, incubated for 1 h at 37°C, and subsequently washed with PBS for 5 min three times; (iii) 140 ml of 3,3',5,5'-tetramethylbenzidine (TMB) chromogenic solution was added into the well containing the samples, and reacted for 10min; subsequently 200 ml of 2M H₂SO₄ was added to stop the reaction; (vi) 150 ml of the reacting solution was transformed into a 96-well plate and was measured at 452 nm.

2.2.2 In vitro testing of blood compatibility

Quantification of adsorbed fibrinogen on the material surface

Fibrinogen is one of the most abundant plasma proteins (4%) and plays an important role in thrombosis²⁰. So the amount of adsorbed fibrinogen on the material surface was measured by direct immunochemistry²¹. Description of the procedure is presented in detail elsewhere¹⁰. Data are normalized to the fibrinogen adsorption to bare 316L SS as 100%.

Quantification of fibrinogen exposed γ -chain on the material surface

The conformational change of fibrinogen, i.e. exposure of γ -chain (HHLGGAKQAGDV at γ 400-411), plays a critical role in fibrin cross-linking, clot formation, and interactions with other molecules²². The amount of exposed γ -chain on the material surfaces was measured by indirect immunochemistry²¹. Description of the procedure is presented in detail elsewhere¹⁰. Data are normalized to the fibrinogen exposing γ -chain to 316L SS as 100%.

Platelet adhesion testing

Platelet-rich plasma (PRP) was prepared by centrifuging (1500rpm, 15min) fresh human whole blood containing 3.8wt% citrate acid solution (blood: citrate acid=9:1) obtained from healthy volunteers, then 50 μ l of fresh PRP was placed onto the sample surface and kept in contact with the surface for 2 h at 37 °C. After incubation, the samples were gently rinsed in PBS to remove loosely adherent platelets from the surface and then they were prepared for subsequent SEM analysis or lactate dehydrogenase (LDH) test.

The samples were fixed by 2 % glutaraldehyde in PBS for 12 h. Then the samples were washed with PBS and dehydrated in a series of increasing ethanol concentrations, then critical point dried and sputter coated with gold for observation using scanning electron microscopy.

The number of adherent platelets was quantified by determining the LDH release after lysis of the cells. A photospectrometric assay based on kinetic determination of the LDH activity was applied. The adherent platelets were lysed by the addition of 40 μ l of 0.1% Triton X-100 to the sample. After 5 mins incubation at room temperature (RT), 25 μ l of each lysate was collected and mixed with 200 μ l mixture solution consisted of 297 μ l of 10 mg/ml reduced nicotinamide adenine dinucleotide (NADH), 187 μ l of 10 mg/ml pyruvate and 10 ml of tris(hydroxymethyl) aminomethane buffer, pH 7.2. The LDH activity in the lysate was then determined by recording the change in absorbance at 340 nm using a microplate photometer. This activity was rated to a lysate of the platelets in the initial PRP in order to quantify the relative number of platelets on each sample.

Platelet activation: P-selectin detection

Surface-induced platelets activation was measured by immunofluorescence method for P-selectin that is expressed on the surface of activated platelets²³. The procedure was as follows: (i) Samples with adherent platelets were fixed with 2% glutaraldehyde in PBS for 1 h and subsequently washed with PBS for 5 min; (ii) 1 ml of 1% sheep serum was added into each well

and incubated for 30 min at 37 °C to block non-specific adsorption; (iii) 30 µl of monoclonal mouse anti-human antibody against P-selectin (1:100) was added onto the sample surfaces, incubated for 2 h at 37 °C, and subsequently washed three times with PBS for 5 min; (iv) monoclonal sheep anti-mouse IgG Cy3-conjugated antibody (1:100) was added to surface of the samples, incubated for 1 h at 37 °C, and subsequently washed with PBS for 5 min three times; (v) the samples were immediately examined with fluorescence microscope with the binning 4×4 and the exposure of 15 s (LEICA DMRX Polarization microscope, Leica, Germany).

2.2.3 In vitro testing of dynamic EPC-compatibility and SMC-compatibility

Isolation and culture of EPCs and SMCs

As previously described, mononuclear cells were separated by density gradient centrifugation (1800r/min, 20min) from the bone marrow of the femur of a SD rat. Mononuclear cells without further purification steps were cultured in Dulbecco's modified Eagle's medium (DMEM) (Gibco BRL, USA) culture medium containing 20 % new born calf serum, 10 ng/ml VEGF, 10ng/ml SCF, penicillin (100 U/ml), and streptomycin sulfate (100 U /ml) at 37°C under 5% CO₂. Cells were fed with fresh medium every third day, and subcultured regularly after the adherent cells reached about 80 % confluence. After 2–3 weeks culturing under VEGF condition, primary mononuclear cells differentiate into endothelial progenitor cells²⁴. Human umbilical artery smooth muscle cells (SMCs) were isolated from newborn umbilical cords as described previously²⁵. Cells in passage 2–5 were used. The SMCs were cultured in DMEM culture medium containing 10 % new born calf serum, penicillin (100 U/ml), and streptomycin sulfate (100 U /ml) at 37°C under 5% CO₂. Cells were fed with fresh medium every third day, and subcultured regularly after the adherent cells reached about 80 % confluence.

Cell attachment of the modified surfaces under dynamic conditions in vitro

Different samples were positioned at the bottom of a parallel wall flow chamber. EPCs or SMCs were re-suspended in DMEM medium containing 10 % fetal calf serum and 50mL of suspensions of EPCs or SMCs at a density of 1×10^6 /mL were perfused into the flow chamber at a shear rate of 1.0 Pa, similar to a small arterial flow. The parallel wall flow chamber was put into a cell incubator (at 37 °C and 5% CO₂). After 2h or 12h incubation, the samples were gently rinsed in PBS to remove loosely adherent cells from the surface. Then, the attached cells onto the samples were determined by an MTT assay and inspected after actin expression using immune-fluorescent

staining¹⁰.

2.2.4 In vitro testing of macrophages compatibility

The murine macrophage cell line RAW264.7 was cultured in DMEM medium containing 10% new fetal calf serum in tissue culture polystyrene flasks. Cells were routinely detached by mechanical force and subsequently split in a ratio of 1:5. The samples with different surfaces were placed into the wells of a 24-well flat-bottomed plate. One milliliter of macrophage suspension at a density of $1 \times 10^5/\text{mL}$ in DMEM medium containing 10% new fetal calf serum were seeded at 37°C for 2 h. After 2h incubation, the samples were gently rinsed in PBS to remove loosely adherent cells from the surface. Then, the adherent macrophages on the different surfaces were analyzed for actin cytoskeleton expression using immune-fluorescent staining.

2.2.5 Statistics

All experiments were performed at least three independent times. All data were compared with one-way ANOVA tests to evaluate statistical significance using SPSS software. Tukey multiple comparisons test was performed as post-hoc test to find significant differences between pairs. A probability values less than 0.05 were considered statistically significant. In the figures, statistically significant differences ($p < 0.05$) were denoted with *.

2.3 Ethics Statement

Fresh human whole blood and newborn umbilical cords obtained from healthy volunteers after informed consent. All animals or human subjects experiments used protocols that were approved by Anhui Medical University (Protocol Number: 20131412).

3 Results and discussion

QCM-D has been applied to monitor the assembly process of each component on gold-coated quartz crystal surface in real time. Mass vs. time curves (Figure 2) clearly demonstrated the buildup process of the coating. Upon injection of DA or SPA or CD34 solution, the crystal frequency decreased (data not shown), indicating the adsorption of the DA or the SPA or the anti-CD34 antibody onto the crystal surface. Determined by Q-Tools software, the adsorbed amounts of DA, SPA and anti-CD34 Ab were $\sim 1152\text{ng}/\text{cm}^2$, $\sim 666\text{ng}/\text{cm}^2$ and $\sim 140\text{ng}/\text{cm}^2$, respectively. Dopamine has been widely used for biomaterials surface modification, as it is easy to obtain abundant active groups (mostly phenolic hydroxyl/o-quinone and amino/imino) for

bimolecular immobilization on material surface with minimal change in the chemical structure of biomaterials²⁶. Here, dopamine was used to bind SPA onto substrate materials. The QCM result indicated that dopamine was successfully immobilized onto 316L SS surface, meanwhile, the dopamine adsorption to the quartz crystal surface was observed as a continuous mass increase with the deposition time and did not come up to the adsorption saturation. Based on the previous studies²⁷, dissolved oxygen and pH induce dihydroxyl group protons in dopamine to deprotonate, oxidizing dopamine to dopaminequinone. When the amine group is deprotonated, the molecule can undergo a 1,4 Michael addition. Further rearrangement leads to 5,6-dihydroxyindole, and the further oxidation causes indolequinone. The reverse dismutation reaction between catechol and o-quinone of 5,6-dihydroxyindole leads to cross linking and formation of polydopamine (self-polymerization), so dopamine could continuously adsorb onto materials with the deposition time. With the deposition time increasing, the polydopamine would cover the substrate materials completely. Then subsequent immobilization of biomolecular would be determined by the polydopamine, so the gold (Au)-coated quartz crystal could approximately exhibit the mass change on the 316L SS surface.

The reverse dismutation reaction between catechol and o-quinone of 5,6-dihydroxyindole can further react with amine groups for binding proteins onto the DA surface²⁶. As the QCM result indicates, this reaction was used successfully to immobilize SPA via the polydopamine coating by simple immersion. SPA interacts with antibodies specifically at their Fc region, which is distant from the antigen binding sites^{11, 14}. The QCM data indicate that the anti-CD34 antibody was successfully immobilized onto 316L SS by simple immersion. Because SPA could lead to oriented immobilization of antibodies and up water was used as solvent and rinsing solution, the activity of anti-CD34 is expected to be maintained. The stability of coating was the most important factor of the technique applied. After being prepared, the coating was rinsed with up water at high flow velocity of 500 $\mu\text{l}/\text{min}$ for 24 hour (Figure 2). No significant mass change indicated that the coating was very stable.

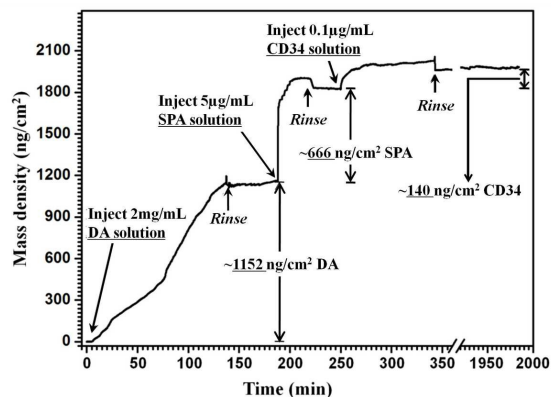


Figure 2. Adsorbed mass changes determined from the QCM-D

The chemical composition of the surfaces at various stages was analyzed by XPS. The survey spectrum and high-resolution C1s and O1s spectra for the SS-DA, SS-DA-SPA and SS-DA-SPA-CD34 are represented in Figure 3. In the survey spectrum of the SS-DA, the presence of N, which were not detected in the surface of 316L SS (data not presented) indicates that dopamine was successfully immobilized onto the surface of 316L SS. Meanwhile, Fe2p and Cr2p peaks disappeared (data not presented), indicating that the dopamine had covered the substrate materials completely, so the mass change of QCM on gold (Au)-coated quartz crystal could approximately exhibit it on the 316L SS surface.

The O1s spectrum for the surfaces at various stages were showed in Figure 3, with BEs at 531.4 eV for the O=C species and 532.9 eV for O-C species(data not presented)²⁶. By calculating peak areas, the molar concentration ratios of O=C/O for the SS-DA, SS-DA-SPA and SS-DA-SPA-CD34 were 38.1%, 49.5% and 44.9%, respectively. The C1s spectrum for the surfaces at various stages were curve-fitted with four peak components, with BEs at 284.5 eV for the C-C/C-H species, 285.5 eV for the C-N species, 286.6 eV for the C-O species and 288.1 eV for the C=O species²⁸. By calculating peak areas, the molar concentration ratios of C=O/C for the SS-DA, SS-DA-SPA and SS-DA-SPA-CD34 were 9.9%, 16.3% and 11%, respectively. The results of O1s and C1s showed that there were more C=O species on the SPA modified surface than other surfaces. The reaserch proved that more than 40% of the amino acid composition of SPA were Asx (asparagine and aspartate) and Glx (glutamine and glutamate) having two carbonyl groups (C=O)²⁹, therefore, the highest molar concentration ratios of C=O/C and O=C/O for SS-DA-SPA indicate that SPA was immobilized onto the dopamine modified surface. After anti-CD34 antibody

grafting to the surface, the molar concentration ratios of C=O/C and O=C/O decreased, confirming the successful immobilization onto the SPA modified surface.

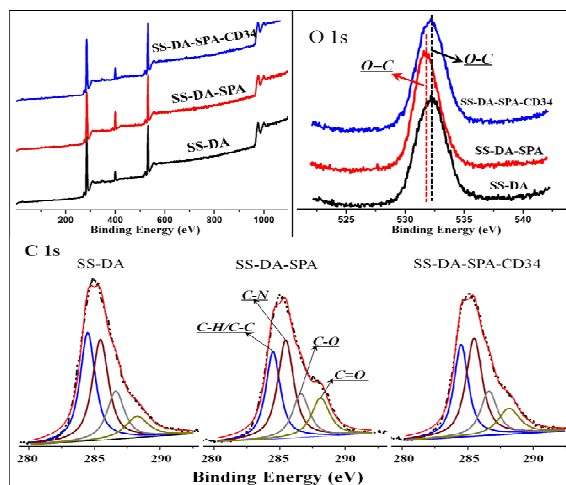


Figure 3. The XPS spectra for different surfaces

The measurement of water contact angle (WCA) is well known as a useful technique to investigate the surface characteristics. WCA of the different surfaces is shown in Figure 4. Compared with 316L SS, the WCA of the DA-modified surface decreased significantly. Relative to the DA-modified surface, the WCA of the SPA surface increased significantly. After anti-CD34 antibody immobilization, the WCA decreased significantly. These results indirect indicated that three types of components were successfully immobilized onto the 316L SS surface step by step.

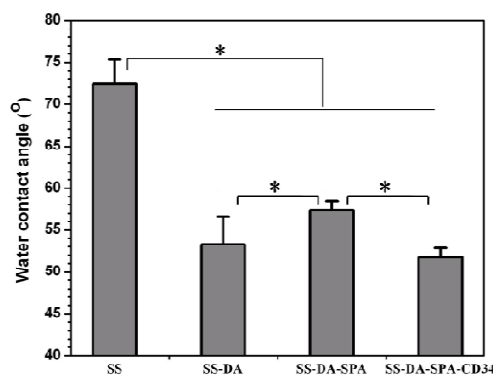


Figure 4. Water contact angle of different surfaces

The amount of F(ab') fragments exposure of anti-CD34 Ab on the surface was determined by ELISA using rabbit anti-Goat IgG F(ab')₂-Peroxidase antibody which react with goat IgG F(ab')₂ but not Fc fragments. The optical density of the anti-CD34 antibody modified surface and the SPA modified surface were measured as 0.134±0.004 and 0.010±0.002, respectively. The data proved

that the oriented immobilization of anti-CD34 antibody was realized by using SPA.

Fibrinogen, one of the most important proteins in the blood coagulation, has several cell adhesion and protein interaction domains. The data of the fibrinogen adsorption on the various surfaces, normalized to the amount on 316L SS, are shown in Figure 5. Compared to 316L SS, the amount of fibrinogen adsorption on other surfaces decreased significantly. One reason for this may be that hydrophilic surface could resist fibrinogen adsorption to some extent³⁰. Fibrinogen adsorption onto SPA surface and CD34 surface was not obviously different.

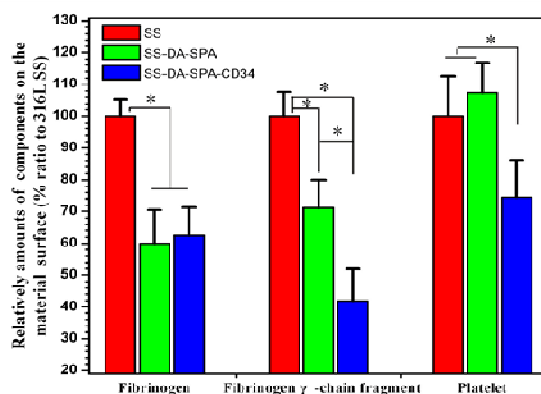


Figure 5. Relative amount of fibrinogen, fibrinogen-exposed γ -chain, and platelets on the material surface compared with 316L SS

Numerous studies have demonstrated that adsorbed fibrinogen on the surface may expose previously hidden γ -chain which mediate fibrin cross-linking, clot formation, and interactions with blood platelets²². The relative amount of fibrinogen with exposed γ -chain on the different surfaces, normalized to the amount on 316L SS, is shown in Figure 5. Compared to 316L SS, the amount of fibrinogen exposed γ -chain on the SPA surface significantly decreased. After anti-CD34 antibody immobilization, the amount of fibrinogen exposed γ -chain further decreased significantly.

The quantitative analysis of platelet adhesion on the different surfaces was performed, by determination of the LDH release after lysis of the adherent blood platelets. The adherent platelets on the CD34 surface were far less than on the 316L SS and the SPA surface (Figure 5), but there was no significant difference for the 316L SS and the SPA surface.

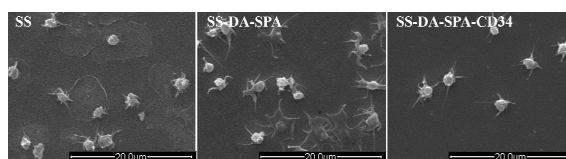


Figure 6. SEM micrographs of platelets adhered on different surfaces

SEM imaging was performed to visualize adherent platelet on the various surfaces (Figure 6). The largest number of adherent platelets was found on the SPA surface, while the least number was found on the CD34 surface. The platelets on the CD34 surface showed generally less pseudopodia or deformation than they on the other surfaces.

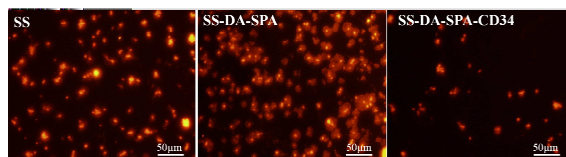


Figure 7. Representative P-selectin stain images showing activated platelets that are labeled with a fluorescent dye.

The surface-induced platelet activation was probed by fluorescent staining for P-selectin (Figure 7); the activated platelets fluorescence red and were much less on the CD34 surface than on the other surfaces. The CD34 surface resisted platelet adhesion and platelet activation better than the other surfaces.

As a blood-contacting biomedical device, the surface should prevent the thrombus formation. In general, when materials contact with blood, proteins are first adsorbed instantaneously onto surfaces and deformed, then platelets are adsorbed, activated and aggregated. Fibrinogen is one of the most important proteins in the blood coagulation. After adsorption, fibrinogen may deformed to mediate thrombus formation²². To estimate surface effect on fibrinogen adsorbed and fibrinogen deformed, the ratio of fibrinogen exposed γ -chain to totally adsorbed fibrinogen was used, which showed an increase in the order: SS-DA-SPA-CD34 < SS < SS-DA-SPA. The higher this ratio, the more fibrinogen adsorbed on this surface had undergone post-adsorptive conformational changes. In proteins adsorption and conformational change processes, surface chemistry is the critical determinant of the exposure of bioactive motifs that are “hidden” within the protein in its native conformation, which then stimulate adverse cellular responses³⁰. The results indicate that the SPA surface induce stronger conformational changes of fibrinogen than 316L SS and the CD34 surface. One reason for this may be that there are the highest molar concentration ratio of -COOH for SS-DA-SPA, because of more than 40% of the acidic amino acid composition of SPA²⁹. A similar result was also seen in another investigation in which neutral and negative surfaces were adsorbed with equivalent amounts of fibrinogen, and neutral surface formed little to no fibrin compared to other surface³¹. In addition, our previous study indicated that

anti-CD34 antibody surface hinder the adsorbed fibrinogen to deform¹⁰.

Platelets play a major role in the initial thrombus formation. Therefore, a study on platelet adhesion and activation is the key step to evaluate the hemocompatibility of materials. The results of platelet adhesion testing and platelet activation indicated that the CD34 surface had good hemocompatibility. One reason for this may be that the least adsorbed fibrinogen had undergone post-adsorptive conformational changes. A similar result was also seen in another investigation in which the CD34 surface had good hemocompatibility³².

It is known from other *in vivo* experiments that true long-term blood compatibility cannot be achieved by simply preventing platelet adhesion^{33, 34}. Recent studies have shown that rapid re-endothelialization at the disease site and on the surface of devices not only provides an inherent antithrombogenic potential but also interrupts cytokine-driven activation of smooth muscle cells (SMCs) leading to restenosis⁵. The concept of rapid re-endothelialization has been developed to immobilize anti-CD34 antibody with specific affinity for EPC on a surface^{8, 13, 35}.

In this study, the anti-CD34 antibody was immobilized onto a material surface. For the purpose of rapid re-endothelialization, the CD34 binding surface must show higher affinity for EPC than for SMC. To evaluate the affinity of the CD34 surface for EPC versus SMC, three types of surface were incubated with EPCs and SMCs under flow conditions for 2h or 12h. Immunofluorescent micrographs of the actin cytoskeleton show that EPCs (Figure 8) and SMCs (Figure 9) grew well on these surfaces. It could be seen in Fig. 9 that the number of adherent EPCs on the CD34 surface was significantly higher than on other surfaces at the initial attachment stage (2 h after seeding) and at the early growth stage (12 h after seeding), which suggested that the anti-CD34 antibody modified 316L SS favored EPC adhesion. However, no difference in adherent SMC numbers could be identified between the materials at the initial attachment stage (2 h after seeding) and at the early growth stage (12 h after seeding), which suggests that the anti-CD34 antibody modified surface did not favor SMC attachment more than other samples.

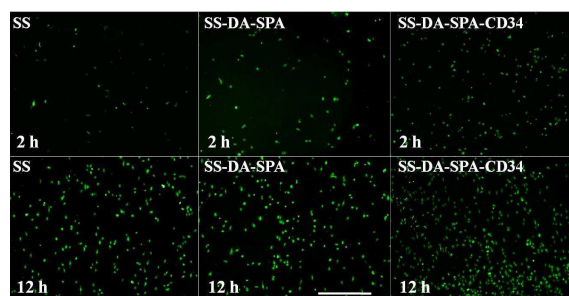


Figure 8. FTIC-immunofluorescent micrographs of actin expression of EPCs adherent on different surfaces under flow conditions for 2h and 12h culture (bar 100 μ m)

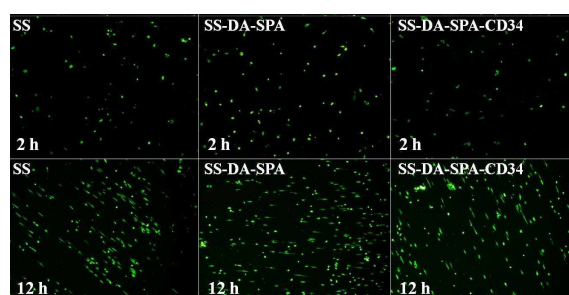


Figure 9. FTIC-immunofluorescent micrographs of actin expression of SMCs adherent on different surfaces under flow conditions for 2h and 12h culture (bar 100 μ m)

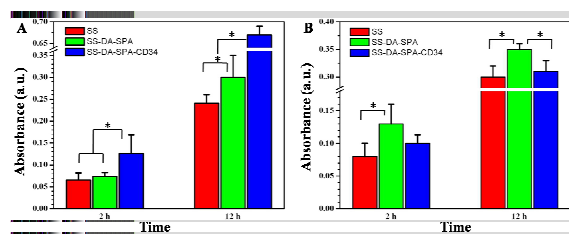


Figure 10 EPCs(A) and SMCs(B) attachment on different surfaces after different culture time measured by MTT assay. n = 5

The effect of anti-CD34 antibody modification on EPC and SMC attachment quantified at 2 h and 12 h by MTT assay (Figure 10). The number of adherent EPCs on the CD34 surface was about twice as many as it on the SPA surface and on the 316L SS surface after 2h incubation. After 12 h culture, the number of adherent EPCs on the CD34 surface was far more than two-fold compared to the SPA surface and the 316L SS surface. Compared with the 316L SS surface, no significant difference of SMC attachment was observed on the CD34 surface after culturing 2h and 12h. The number of adherent SMCs on the SPA surface is more than it on the other surfaces. This confirms that the CD34 surface has highly affinity for EPC rather than SMC and is favorable for rapid re-endothelialization.

Though this anti-CD34 modified surface was unable to resist SMCs attachment compared with 316L SS, it could significantly promote EPCs attachment. Continuous supplement of EPC from blood could ensure that the surface was covered rapidly by EPC, because the time needed for SMC proliferation should be longer than the time needed for EPC attachment. The clinical application of the anti-CD34-coated Genous™ Bio-engineered R stent (OrbusNeich, Hong Kong) indicated that capturing of EPCs on a surface could promote rapid re-endothelialization and inhibit SMCs proliferation and thromboresistance³⁶.

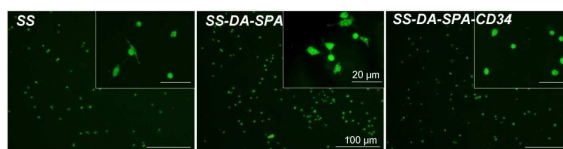


Figure 11. FTIC-immunofluorescent micrographs of actin cytoskeleton of macrophages adherent on different surfaces for 2h culture

To study the biocompatibility of biomaterials, the behavior of macrophages is useful to be determined. The use of macrophages for this purpose is based on their role in the foreign body response³⁷. Macrophages adhered on the every surfaces were stained for their actin cytoskeleton and shown in Figure 11. The results show that the macrophage population on the CD34 surface was significantly less than on the SPA surface, meanwhile, macrophages extended pseudopods and frontal cytoplasmic fringe or presented an irregular shape on the 316L SS surface and the SPA surface, while less pseudopods extended or rounded shape emerged for macrophages on the CD34 surface. This implies that the CD34 surface induces lower local inflammation reaction and restenosis after implantation.

4 Conclusions

Polydopamine-Staphylococcal Protein A coating is an effective method for oriented immobilization of antibodies. This was demonstrated here with immobilization of endothelial progenitor cell capturing anti-CD34 antibodies. Preferential binding of EPC compared to SMC could be shown under flow conditions, the antibody modified surface also induced less adhesion of macrophages, showing a low inflammatory potential. Also other properties indicated a good hemocompatibility: The surfaces adsorbed less fibrinogen compared to bare stainless steel and induced less fibrinogen denaturation than the DA-SPA surface without antibody. These properties promise a good suitability of the treatment for stent coating.

Acknowledgments

This work was supported by Natural Science Foundation of China (No.31300792), China Postdoctoral Science Foundation (No.2014M561813), Natural Science Foundation of Anhui Province (No.1408085QH149). This work was supported by Grants for Scientific Research of BSKY(XJ201232) from Anhui Medical University.

References

1. L. Xue and H. P. Greisler, *J Vasc Surg*, 2003, **37**, 472-480.
2. C. Werner, M. F. Maitz and C. Sperling, *J Mater Chem*, 2007, **17**, 3376-3384.
3. J. E. Sousa, P. W. Serruys and M. A. Costa, *Circulation*, 2003, **107**, 2274-2279.
4. D. W. Losordo, J. M. Isner and L. J. Diaz-Sandoval, *Circulation*, 2003, **107**, 2635-2637.
5. V. J. Dzau, D. Kong, L. G. Melo, A. A. Mangi, L. Zhang, M. Lopez-Illasaca, M. A. Perrella, C. C. Liew and R. E. Pratt, *Circulation*, 2004, **109**, 1769-1775.
6. T. Asahara, T. Murohara, A. Sullivan, M. Silver, R. vanderZee, T. Li, B. Witzenbichler, G. Schatteman and J. M. Isner, *Science*, 1997, **275**, 964-967.
7. Chen J.L., Li Q.L., Chen J.Y. and H. N., *Advanced Materials Research*, 2008, **47-50**, 1411-1414.
8. J. Aoki, A. T. L. Ong, E. P. McFaden, W. J. van der Giessen, G. Sianos, E. Regar, P. de Feyter, M. J. B. Kutryk and P. W. Serruys, *Journal of the American College of Cardiology*, 2005, **45**, 69a-69a.
9. Q. Lin, X. Ding, F. Qiu, X. Song, G. Fu and J. Ji, *Biomaterials*, 2010, **31**, 4017-4025.
10. J. Chen, J. Cao, J. Wang, M. F. Maitz, L. Guo, Y. Zhao, Q. Li, K. Xiong and N. Huang, *J Colloid Interf Sci*, 2012, **368**, 636-647.
11. B. Lu, M. R. Smyth and R. O'Kennedy, *Analyst*, 1996, **121**, 29R-32R.
12. C. M. Halliwell, *Analyst*, 2004, **129**, 1166-1170.
13. Q. L. Li, N. Huang, C. Chen, J. L. Chen, K. Q. Xiong, J. Y. Chen, T. X. You, J. A. Jin and X. Liang, *J Biomed Mater Res A*, 2010 **94A**, 1283-1293.
14. N. Tajima, M. Takai and K. Ishihara, *Anal Chem*, 2011, **83**, 1969-1976.
15. A. P. Le Brun, S. A. Holt, D. S. Shah, C. F. Majkrzak and J. H. Lakey, *Biomaterials*, 2011, **32**, 3303-3311.
16. H. Lee, S. M. Dellatore, W. M. Miller and P. B. Messersmith, *Science (New York, N.Y.)*, 2007, **318**, 426-430.
17. J. G. Rivera and P. B. Messersmith, *J Sep Sci*, 2012, **35**, 1514-1520.
18. D. E. Fullenkamp, J. G. Rivera, Y. K. Gong, K. H. Lau, L. He, R. Varshney and P. B. Messersmith, *Biomaterials*, 2012, **33**, 3783-3791.
19. T. S. Sileika, H. D. Kim, P. Maniak and P. B. Messersmith, *ACS Appl Mater Interfaces*, 2011, **3**, 4602-4610.
20. R. Murthy, C. E. Shell and M. A. Grunlan, *Biomaterials*, 2009, **30**, 2433-2439.
21. T. Y. Ning, X. H. Xu, L. F. Zhu, X. P. Zhu, C. H. Chu, L. K. Liu and Q. L. Li, *Journal of biomedical materials research. Part B, Applied biomaterials*, 2012, **100**, 138-144.
22. M. W. Mosesson, *Journal of Thrombosis and Haemostasis*, 2003, **1**, 231-238.
23. J. L. Chen, Q. L. Li, J. Y. Chen, C. Chen and N. Huang, *Applied Surface Science*, 2009, **255**, 6894-6900.

24. J. Chen, C. Chen, Z. Chen, J. Chen, Q. Li and N. Huang, *J Biomed Mater Res A*, 2010, **95A**, 341-349.
25. P. K. Vadiveloo, H. R. Stanton, F. W. Cochran and J. A. Hamilton, *Artery*, 1994, **21**, 161-181.
26. L. Lu, Q. L. Li, M. F. Maitz, J. L. Chen and N. Huang, *J Biomed Mater Res A*, 2012, **100**, 2421-2430.
27. Y. Weng, Q. Song, Y. Zhou, L. Zhang, J. Wang, J. Chen, Y. Leng, S. Li and N. Huang, *Biomaterials*, 2011, **32**, 1253-1263.
28. F. J. Xu, Q. J. Cai, Y. L. Li, E. T. Kang and K. G. Neoh, *Biomacromolecules*, 2005, **6**, 1012-1020.
29. Q. L. Li, N. Huang, J. Chen, G. Wan, A. Zhao, J. Chen, J. Wang, P. Yang and Y. Leng, *J Biomed Mater Res A*, 2009, **89**, 575-584.
30. B. Sivaraman, K. P. Fears and R. A. Latour, *Langmuir*, 2009, **25**, 3050-3056.
31. K. M. Evans-Nguyen, L. R. Tolles, O. V. Gorkun, S. T. Lord and M. H. Schoenfish, *Biochemistry-Us*, 2005, **44**, 15561-15568.
32. A. Tan, D. Goh, Y. Farhatnia, N. G. J. Lim, S. H. Teoh, J. Rajadas, M. S. Alavijeh and A. M. Seifalian, *PloS one*, 2013, **8**, e77112.
33. M. Albers, V. M. Battistella, M. Romiti, A. A. E. Rodrigues and C. A. B. Pereira, *J Vasc Surg*, 2003, **37**, 1263-1269.
34. P. Libby, M. Nahrendorf, M. J. Pittet and F. K. Swirski, *Circulation*, 2008, **117**, 3168-3170.
35. J. I. Rotmans, J. M. M. Heyligers, H. J. M. Verhagen, E. Velema, M. M. Nagtegaal, D. P. V. de Kleijn, F. G. de Groot, E. S. G. Stroes and G. Pasterkamp, *Circulation*, 2005, **112**, 12-18.
36. S. Silber, P. Damman, M. Klomp, M. A. Beijk, M. Grisold, E. E. Ribeiro, H. Suryapranata, J. Wojcik, K. Hian Sim, J. G. Tijssen and R. J. de Winter, *EuroIntervention : journal of EuroPCR in collaboration with the Working Group on Interventional Cardiology of the European Society of Cardiology*, 2011, **6**, 819-825.
37. T. Futami, N. Fujii, H. Ohnishi, N. Taguchi, H. Kusakari, H. Ohshima and T. Maeda, *Journal of Periodontology*, 2000, **71**, 287-298.

Graphical Abstract:

